# IMMISCIBLE-INTERFACE ASSISTED DIRECT METAL DRAWING

Li He[1,2], Fan Fei[1,2], Wenbo Wang[1,2], Xuan Song[1,2*]

[1]Department of Industrial and Systems Engineering, University of Iowa, Iowa City, IA
52242, USA
2 Center for Computer Aided Design, University of Iowa, Iowa City, IA 52242, USA

## Abstract

State-of-the-art metal additive manufacturing (AM) techniques construct a three-dimensional (3D) structure through sintering or melting dry metal powders in a layer-by-layer fashion, which consequently results in some typical manufacturing defects in the final structure, such as residual stress and highly-orientated microstructures. To overcome these defects, we present a new low-cost metal AM process, named Immiscible-interface assisted Direct Metal Drawing (II-DMD), which fabricates self-supported and isotropic 3D metal structures by continuously extruding a metal colloidal suspension within a second immiscible matrix colloidal suspension. The shape of the metal colloidal suspension is stabilized due to the presence of an immiscible interface between the two colloidal suspension systems. Dense metal structures can be achieved via post-consolidation of the self-stabilized metal-matrix systems, including liquid-phase drying and metal-phase sintering. In this article, the immiscible-interface-assisted self-stabilization mechanism is studied. The post-consolidation processes are discussed. Several test cases were fabricated and characterized.

**Keywords:** immiscible interface, direct metal drawing, colloidal suspension, self-stabilization, heat treatment

## 1. Introduction

Traditional metal additive manufacturing (AM) processes [1] build a three-dimensional (3D) metallic structure through selectively sintering or melting dry metal powders in a layer-by-layer manner using a high-energy beam. The layerwise fabrication method used in those processes results in many typical manufacturing defects in final structures, such as the staircase effect, residual stress and highly-orientated microstructures. Specifically, the staircases can reduce the surface finish and introduce stress concentration; residual stress and highly-orientated microstructures caused by the localized high-temperature heating [2, 3] reduce mechanical properties of final objects. In addition to these drawbacks, fabrication costs of existing metal AM processes are substantially high, due to required high-energy sources, which limit broader application in industry.

In this paper, we report a new AM process for fabricating metallic structures ( in particular lattice structures), i.e., immiscible-interface assisted direct metal drawing (II-DMD), which offers the potential to mitigate the inherent defects associated with layerwise fabrication approaches. In this new process, a metal-powder-based suspension is first deposited continuously in 3D space

---

* Corresponding author.

within a secondary matrix suspension and then uniformly densified through heat treatment. By tailoring the two colloidal systems, a suitable immiscible interface can be established between the metal-powder suspension and the secondary matrix suspension, which consequently enables the self-stabilization of the deposited 3D geometry. Similar fabrication techniques [4-12] have been used to create microvascular networks[12], soft sensors[10], robots[11], and other 3D structures, which are however still limited to polymer materials (e.g. hydrogel) and have not yet been attempted to build metal structures. The paper is organized as follows. Section 2 describes starting materials used in the II-DMD process; section 3 introduces a fabrication system; section 4 discusses a mathematic model for the nozzle extrusion of the II-DMD process; section 5 demonstrates several test cases and their properties; conclusions and future work are discussed in section 6.

## 2. Starting materials

In this research, bronze powders are used as a model material to study the II-DMD process. Aluminum oxide is selected to form a secondary matrix suspension due to its high sintering temperature (> 1300ºC). Bronze-powder-based suspensions are prepared by mixing as-received bronze powders (10% Tin, 90% Copper and 0.07% Phosphor, Mesh: 325, Chemical Store Inc. Clifton, NJ, USA) with silicone oil at a specific concentration in a magnetic stirrer for ~15 minutes. The resulting bronze-powder suspension needs to exhibit a shear-thinning behavior with yield stress to achieve controllable extrusion through a pressurized dispenser. Moreover, the shear elastic modulus and yield stress of the achieved bronze-powder suspension should be an order of magnitude larger than those of the used secondary matrix suspension to ensure that the suspension maintains its shape after it exits the nozzle [13]. A secondary matrix colloidal suspension is prepared by mixing alumina powder (GE6, Baikowski, Charlotte, USA) with deionized water at a specific concentration in a magnetic stirrer for ~15 minutes. Similarly, the achieved matrix suspension should exhibit a shear-thinning behavior with suitable yield stress to support the extruded bronze-powder suspensions [14]. Additionally, the matrix suspension needs to be thixotropic such that crevices generated by nozzle movement can be immediately closed through a time-dependent backflow.

Silicon oil and water are employed as the dispersion medium of metal suspensions and secondary matrix suspensions respectively to introduce an immiscible interface [15, 16] between bronze particles and alumina particles, which is required to achieve the self-stabilization of a deposited 3D shape. More details are discussed in section 3.

## 3.  Process Design

A schematic representation of the II-DMD process is shown in Figure 1. A pressurized dispensing syringe is mounted on a three degrees of freedom (DoF) gantry system. The syringe is loaded with a bronze-powder suspension and is controlled to continuously dispense the suspension within an alumina matrix suspension in a crucible, as depicted in Figure 1a.1. As the bronze-powder suspension is deposited, an immiscible water-oil interface is established between the bronze and alumina particles, which locks the bronze and alumina particles in position and maintain the 3D shape of the deposited bronze-powder suspension, as shown in Figure 1a.2.

Rheological properties of each suspension have been carefully tailored to avoid deformation of the deposited 3D shape during the fabrication (e.g., fragments, bead up, diffusion, or sedimentation).

After a bronze-powder suspension with the desired geometry is achieved, the crucible is heated in an oven to dry the bronze-powder and alumina-matrix suspensions. The drying schedule is given in Figure 1b. Through this step, a dry bronze-powder compact with the desired geometry is formed, surrounded by a nearly dry alumina powder bed (refer to Figure 1a.3). The alumina powder bed still contains a small amount of silicon oil that diffused from the bronze-powder suspension during drying. After that, both the bronze-powder compact and the alumina powder bed are heated together in an argon furnace. The heating temperature schedule is given in Figure 1c. Since the used temperature (i.e., 950 ℃) is much lower than the sintering temperature of alumina powder (e.g., 1400 ℃), only bronze particles are sintered/melted, with the alumina matrix powder remaining loose. In addition, during the high temperature sintering, the residual silicone oil in the alumina powder bed is also decomposed. Finally, the alumina matrix powder is removed and recycled for future use, leaving the sintered bronze body as the final product.
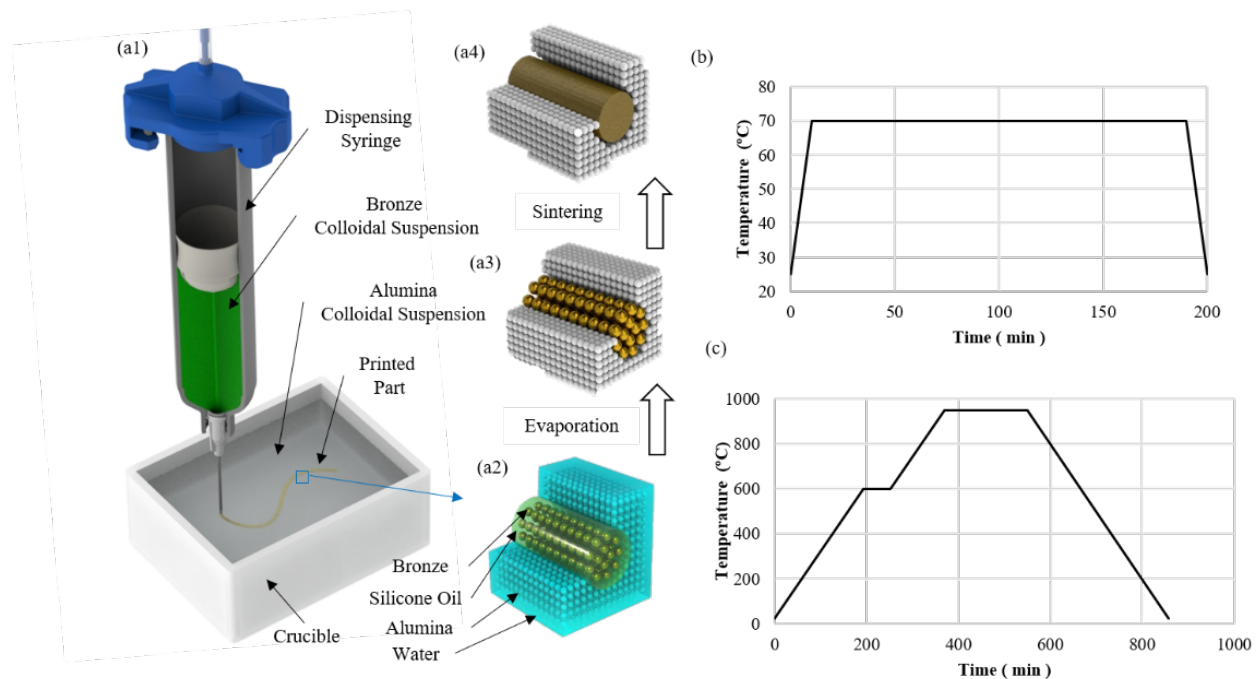


Figure 1. (a) Schematic diagram of II-DMD; (b) temperature schedule for drying; (c) temperature schedule for sintering.

## 4. Process Modeling

The required solid loadings of bronze-powder suspensions and alumina matrix suspensions in the II-DMD process were experimentally determined as 94wt% and 40wt%, respectively, which yield the optimal stability and printability during the process. These materials were used to study the relationship between extrusion pressures, printing speed and extruded filament size (with a fixed nozzle size of 20 Gauge). Figure 2 shows the experimental results and fitting models.

As seen in Figure 2a, the achieved metal filament size in an alumina powder bed after drying is proportional to the applied extrusion pressure. In contrast, the achieved metal filament size is inversely proportional to the square root of printing speed, as shown in Figure 2b. Based on the experimental results, bronze filament sizes achieved through a 20 Gauge nozzle can be expressed as the following equation:

$$y \approx 250\sqrt{2} * p * v^{-0.5}$$ (1)

In which:

- $y$ is the filament size (unit: $\mu m$);
- $p$ is the extrusion pressure (unit: $psi$);
- and $v$ is the nozzle printing speed (unit: $mm/s$).
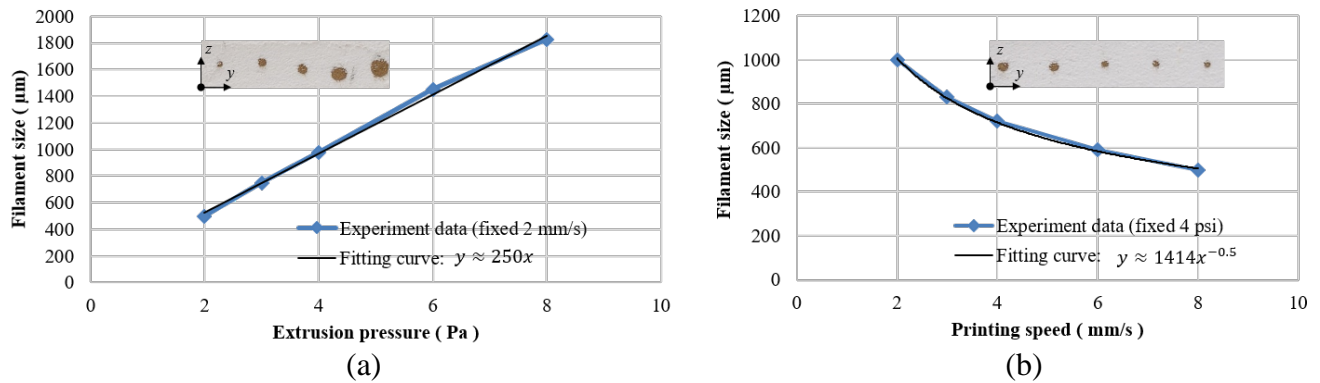


Figure 2. Effects of (a) extrusion pressure and (b) printing speed on extruded filament size.

## 5. Test Cases

In this section, several test cases were fabricated to showcase the presented II-DMD process. Figure 3a shows a bronze lattice structure, which can be used as structural frames of micro robots. Figure 3b shows a stent structure, which can be applied to prop up a pathological changed blood vessel in the human body if shape memory alloy powder is used.

To further demonstrate the capability of the II-DMD process, two cone springs with different sizes were printed and shown in Figure 3c. An optical microscope image of the external surface of the springs is shown in Figure 3d. The rough surface finish is mainly caused by a large bronze particle size used in the process. SEM images of the spring specimens are shown in Figure 3e and 3f. It can be seen that small pores with diameters around 10 to 40 $\mu m$ exist in the cross section, which may be caused by inappropriate selection of bronze particle size and drying parameters. In Figure 3f, the metal cross section is dense at a macroscopic level, which contributes to relatively good mechanical properties of printed parts. According to a tensile test as shown in Figure 3g, bronze specimens fabricated by our method have a yield strength of 106 MPa and an ultimate strength of 148 MPa.
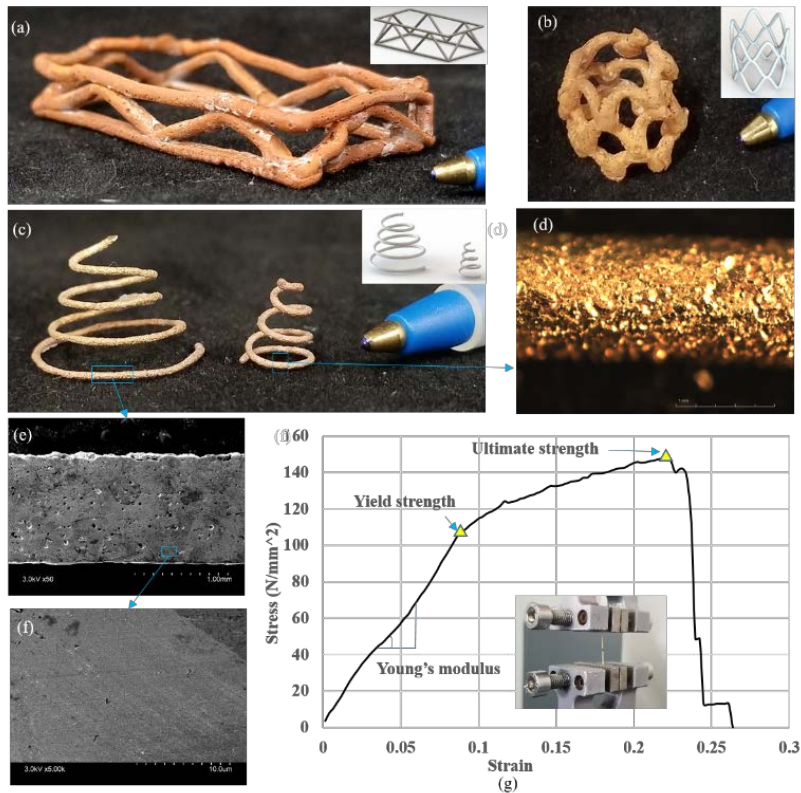
Figure 3. Test cases: (a) a lattice structure, (b) stent structure, (c) cone springs, (d) optical microscope image of springs, (e) and (f) SEM images of printed samples, (g) tensile test of a fabricated specimen.

## 6. Conclusion and Future Work

In this article, we report a new and low-cost metal 3D printing process, in which an immiscible interface and unique rheological behaviors of highly-loaded metal and ceramic colloidal suspensions are utilized to build complex metal lattice structures. It can potentially fabricate numerous metal materials without generating staircase effect and the need of support structures, and the microstructures of achieved metal parts can be homogeneous and isotropic. Bronze materials are used as a model material to demonstrate the process, with alumina powder as a matrix material. In the future, problems such as rough surface finish and porosity still need to be solved. Fundamental physics behind the II-DMD process will be studied and more materials will be tested.

## References

[1]     Gu, D., Meiners, W., Wissenbach, K., and Poprawe, R., 2012, "Laser additive manufacturing of metallic components: materials, processes and mechanisms," International materials reviews, 57(3), pp. 133-164.

[2]     Strößner, J., Terock, M., and Glatzel, U., 2015, "Mechanical and Microstructural Investigation of Nickel-Based Superalloy IN718 Manufactured by Selective Laser Melting (SLM)," Advanced Engineering Materials, 17(8), pp. 1099-1105.

[3]     Chen, H., Gu, D., Dai, D., Ma, C., and Xia, M., 2017, "Microstructure and composition homogeneity, tensile property, and underlying thermal physical mechanism of selective laser melting tool steel parts," Materials Science and Engineering: A, 682, pp. 279-289.

[4]     Bhattacharjee, T., Zehnder, S. M., Rowe, K. G., Jain, S., Nixon, R. M., Sawyer, W. G., and Angelini, T. E., 2015, "Writing in the granular gel medium," Science Advances, 1(8).

[5]     Esser-Kahn, A. P., Thakre, P. R., Dong, H., Patrick, J. F., Vlasko-Vlasov, V. K., Sottos, N. R., Moore, J. S., and White, S. R., 2011, "Three-Dimensional Microvascular Fiber-Reinforced Composites," Advanced Materials, 23(32), pp. 3654-3658.

[6]     Grosskopf, A. K., Truby, R. L., Kim, H., Perazzo, A., Lewis, J. A., and Stone, H. A., 2018, "Viscoplastic Matrix Materials for Embedded 3D Printing," ACS Applied Materials & Interfaces.

[7]     Hanson Shepherd, J. N., Parker, S. T., Shepherd, R. F., Gillette, M. U., Lewis, J. A., and Nuzzo, R. G., 2011, "3D microperiodic hydrogel scaffolds for robust neuronal cultures," Advanced functional materials, 21(1), pp. 47-54.

[8]     Moravej, M., and Mantovani, D., 2011, "Biodegradable metals for cardiovascular stent application: interests and new opportunities," International journal of molecular sciences, 12(7), pp. 4250-4270.

[9]     Subramanian, V., Fréchet, J. M., Chang, P. C., Huang, D. C., Lee, J. B., Molesa, S. E., Murphy, A. R., Redinger, D. R., and Volkman, S. K., 2005, "Progress toward development of all-printed RFID tags: materials, processes, and devices," Proceedings of the IEEE, 93(7), pp. 1330-1338.

[10]    T., M. J., M., V. D., L., T. R., Yiğit, M., B., K. D., J., W. R., and A., L. J., 2014, "Embedded 3D Printing of Strain Sensors within Highly Stretchable Elastomers," Advanced Materials, 26(36), pp. 6307-6312.

[11]    Wehner, M., Truby, R. L., Fitzgerald, D. J., Mosadegh, B., Whitesides, G. M., Lewis, J. A., and Wood, R. J., 2016, "An integrated design and fabrication strategy for entirely soft, autonomous robots," Nature, 536, p. 451.

[12]    Willie, W., Adam, D., and A., L. J., 2011, "Omnidirectional Printing of 3D Microvascular Networks," Advanced Materials, 23(24), pp. H178-H183.

[13]    Muth, J. T., Vogt, D. M., Truby, R. L., Mengüç, Y., Kolesky, D. B., Wood, R. J., and Lewis, J. A., 2014, "Embedded 3D printing of strain sensors within highly stretchable elastomers," Advanced Materials, 26(36), pp. 6307-6312.

[14]    He, L., and Song, X., 2018, "Supportability of a High-Yield-Stress Slurry in a New Stereolithography-Based Ceramic Fabrication Process," JOM, 70(3), pp. 407-412.

[15]    Paunov, V. N., Al-Shehri, H., and Horozov, T. S., 2016, "Attachment of composite porous supra-particles to air–water and oil–water interfaces: theory and experiment," Physical Chemistry Chemical Physics, 18(38), pp. 26495-26508.

[16]    Sharp, E. L., Al-Shehri, H., Horozov, T. S., Stoyanov, S. D., and Paunov, V. N., 2014, "Adsorption of shape-anisotropic and porous particles at the air–water and the decane–water interface studied by the gel trapping technique," RSC Advances, 4(5), pp. 2205-2213.